Real-Time, In Vivo Measurement of Protein Kinase A Activity in Deep Brain Structures Using Fluorescence Lifetime Photometry (FLiP)

Bart Lodder,[1,2] Suk Joon Lee,[1] and Bernardo L. Sabatini[1,3]

[1]Howard Hughes Medical Institute, Department of Neurobiology, Harvard Medical School, Boston, Massachusetts
[2]Department of Translational Neuroscience, Brain Center Rudolf Magnus, University Medical Center Utrecht, Boston, Massachusetts
[3]Corresponding author: *bernardo_sabatini@hms.harvard.edu*

The biochemical state of neurons, and of cells in general, is regulated by extracellular factors, including neurotransmitters, neuromodulators, and growth hormones. Interactions of an animal with its environment trigger neuromodulator release and engage biochemical transduction cascades to modulate synapse and cell function. Although these processes are thought to enact behavioral adaption to changing environments, when and where in the brain they are induced has been mysterious because of the challenge of monitoring biochemical state in real time in defined neurons in behaving animals. Here, we describe a method allowing measurement of activity of protein kinase A (PKA), an important intracellular effector for neuromodulators, in freely moving mice. To monitor PKA activity in vivo, we use a genetically targeted sensor (FLIM-AKAR) and fluorescence lifetime photometry (FLiP). This article describes how to set up a FLiP system and obtain robust recordings of net PKA phosphorylation state in vivo. The methods should be generally useful to monitor other pathways for which fluorescence lifetime reporters exist.

Basic Protocol 1: Building a FLiP system
Basic Protocol 2: FLIM-AKAR viral injection and fiber implantation for FLiP measurement
Basic Protocol 3: Performing measurements using FLiP

Keywords: FLiP • fluorescence • lifetime • photometry • PKA

How to cite this article:
Lodder, B., Lee, S. J., & Sabatini, B. L. (2021). Real-time, in vivo measurement of protein kinase A activity in deep brain structures using fluorescence lifetime photometry (FLiP). *Current Protocols*, *1,* e265. doi: 10.1002/cpz1.265

INTRODUCTION

Behavior of animals is driven by neuronal activity, which changes in response to the environment and an animal's internal state. Changes in the brain happen on the system/circuit, cellular, and molecular levels, and it is by investigating these change processes that the field has aimed to understand neurological function and dysfunction and develop intervention strategies. In the last decades, great progress has been made in developing techniques for investigating the functional relationship between changes in neuronal activity and behavior, such as fiber photometry (Cui et al., 2013), optogenetics (Boyden, Zhang,

CURRENT PROTOCOLS
A Wiley Brand
Current Protocols e265, Volume 1
Published in Wiley Online Library (wileyonlinelibrary.com).
doi: 10.1002/cpz1.265

Bamberg, Nagel, & Deisseroth, 2005; Kim, Adhikari, & Deisseroth, 2017), endoscopic imaging (Barretto, Messerschmidt, & Schnitzer, 2009), and in vivo electrophysiology (Hong & Lieber, 2019). Furthermore, real-time analysis of biochemical signaling, exploiting the many fluorescent sensors that exist for intracellular signaling molecules, has been used in vitro for analysis of dissociated neurons and brain slices (Chen, Saulnier, Yellen, & Sabatini, 2014; Lee, Escobedo-Lozoya, Szatmari, & Yasuda, 2009; Tang & Yasuda, 2017). However, our understanding of the dynamics of molecular changes during behavior traditionally relied on post hoc approaches, which allows for interpretation of molecular changes many minutes after the behavior occurred. Such approaches may be sufficient to investigate long-term and persistent molecular changes; however, more transient molecular changes in response to behavior will not be captured (Ramos et al., 2003). In vivo two-photon (2P) fluorescence lifetime microscopy (FLIM) has been used for continuous imaging of biochemical state in vivo (Díaz-García et al., 2017; Laviv et al., 2020; Ma et al., 2018), but this powerful approach is challenging, mainly applicable to analysis of superficial neurons, and restricted to head-restrained behaviors. Therefore, to investigate the molecular changes during behavior in deep brain areas, we built on previous deep brain fluorescence-based approaches (Cui et al., 2014; Goto et al., 2015) and developed single-fiber fluorescence lifetime photometry (FLiP) (Lee, Chen, Lodder, & Sabatini, 2019, 2020), which allows for continuous lifetime monitoring while an animal is behaving.

FLiP is versatile, and there are many lifetime-based sensors available for use (any Forster resonance energy transfer, or FRET, sensor should be suitable for lifetime-based measurements) (Yasuda, 2018). Furthermore, many classes of sensors exist, some relying on purely intramolecular conformational changes and other exploiting intermolecular interactions. In this article, we describe how to build a FLiP system and apply it to measure the protein kinase A (PKA) pathway in vivo. PKA is a central intracellular effector protein that regulates plasticity (Iino et al., 2020; Yagishita et al., 2014), excitability (Lee et al., 2003; Skeberdis et al., 2006), and gene expression (Lau, Saha, Faris, & Russek, 2004; Nayak, Zastrow, Lickteig, Zahniser, & Browning, 1998). Notably, it is regulated through G-protein-coupled receptors (GPCRs) signaling through $G_{\alpha s/olf}$ or $G_{\alpha i}$ to modulate cAMP levels, thus allowing dynamic modulation through multiple neurotransmitters, such as dopamine (Kebabian, Petzold, & Greengard, 1972; Lee et al., 2020), adenosine (Zhang et al., 2019), or acetylcholine (Nagai, Yoshimoto, Kannon, Kuroda, & Kaibuchi, 2016). In addition, in many cells, PKA is also regulated following activation of Ca^{2+}-sensitive adenylyl cyclase (Linden & Ahn, 1999), which may respond to Ca^{2+} release from intracellular stores or entry through the plasma membrane. The FLiP method allows for the measurement of activity of PKA in genetically targeted cells in a freely moving animal over long time scales, is relatively affordable, and is easy to implement. In addition, FLiP can be used in combination with many other techniques, such as optogenetics, fiber photometry, and pharmacological studies (Lee et al., 2020). Basic Protocol 1 describes how to assemble the optical components to build a FLiP system. In addition, we address considerations for stereotactic FLIM-AKAR viral injection and fiber placement (Basic Protocol 2) and for behavioral task design and data analysis (Basic Protocol 3).

CAUTION: Please handle optical and electrical equipment carefully. Make sure to wear gloves and use lens paper. Additionally, release any static electricity buildup before handling electronic components. Make sure not to expose the hybrid photomultiplier tube (PMT) to ambient light. When using optical equipment, always make sure to follow your institution's safety regulations.

NOTE: Follow all guidelines and regulations with regards to safe animal handling and welfare.

BUILDING A FLiP SYSTEM

The following protocol describes the components, assembly process, and software installation necessary to build a FLiP system capable of measuring fluorescence lifetime in vivo through a fiber optic. Whenever possible, we highlight considerations necessary to achieve an accurate measurement. The system used in our prior work is built using a Becker & Hickl (B&H) SPC 830 time-correlated single-photon counting (TSPC) module. This board is no longer available but is exchangeable for other TSPC modules available from B&H, such as the SPC-150NX. In addition, there are alternative boards that can be used based on field-programmable gate arrays (FPGAs) (Díaz-García et al., 2021). Although our measurements have been performed using custom software, we recommend using the B&H TSPC software, as it has similar functionality and is more user friendly.

Materials

See Table 1.

NOTE: In this protocol, terms indicating orientation (left, right) will be used from the perspective of the propagating laser beam.

NOTE: Part numbers referenced in this protocol can be found in Table 1.

Assembly of the laser, mirror, and kinematic cube

1. Request that a machine shop produce a custom metal plate that secures the base of the laser to the breadboard (42): the base plate (L: 1.575″, W: 4.724″, H: 0.375″) contains four M3 0.5 taps and an 8-32 tap for securing the base plate to the laser and 0.5″ post, respectively. In addition, request that a machine shop produce a metal 30-mm cage plate adapter (43): the 30-mm cage plate adapter (L: 1.5″, W: 1.5″, H: 0.365″) contains two 0.225″ taps and two 4-40 taps for mounting of the plate to the laser and the 30-mm cage system, respectively.

   For more details on the custom mounts and a 3D exploded model of the FLiP system as depicted in Figures 1C and 1D, see GitHub (https://github.com/bernardosabatinilab/fluorescence-lifetime-photometry).

2. Place breadboard (17) on a stable surface.

   It is recommended to build the set-up either on a movable cart or at the intended place of measurement to decrease the risk of damage during transportation.

3. Attach two custom mounts from step 1 (42 and 43) to the base and front of the laser head (1).

4. Screw a 0.5″ post (28) into base of the laser head using the 8-32 setscrew included with the post. Slide 0.5″ post into a post holder (27).

5. Attach laser head (1) to the laser driver and connect power supply using the laser accessory set (2) as directed by the laser manual. Do not turn laser on.

6. Secure laser head on the breadboard using a 1/4″-20 cap screw (29) with the hex key tool set (46). Adjust height of the laser to ∼3.5″, measured from the top of the breadboard to the bottom of the custom laser mount.

7. Attach two 1.5″-long 6-mm rods (22) to front of the laser (one in the bottom and one in a top slot, diagonal from each other) using 4-40 setscrews (30).

8. Screw a 1″ adjustable lens tube (32, external threads, 0.5″ long) into front of the mounted neutral-density (ND) filter (18). Then, secure mounted ND filter to the two rods, with the lens tube facing and fully covering the front opening of the laser head.

Table 1 Materials Needed to Build and Test the FLiP Set-Up (Basic Protocol 1)

#	Material[a]	# needed	Product number	Company
1	473 nm cooled picosecond diode laser, 80 MHz	1	BDS-SM-473-FBC	Becker & Hickl
2	Accessory Set for BDS-Laser	1	CSET-ST-BDS	Becker & Hickl
3	Hybrid PMT	1	HPM-100-07-Cooled	Becker & Hickl
4	Detector controller board	1	DCC-100-PCI	Becker & Hickl
5	Photon counting board	1	SPC-150NX	Becker & Hickl
6	200 µm core patch cord	1	MFP_200/220/900-0.37_3m_FCM-MF1.25	Doric Lenses
7	Low autofluorescence optic implantable fiber	1	MFC_200/230-0.37_4.5 mm_MF1.25_FLT	Doric Lenses
8	488 nm laser BrightLine® single-edge laser dichroic beamsplitter	1	Di02-R488-25 × 36	Semrock
9	517/20 nm BrightLine® single-band bandpass filter	1	FF01-517/20-25	Semrock
10	Kinematic Fluorescence Filter Cube, 30 mm Cage Compatible, Left-Turning, 1/4″-20 Tapped Holes	1	DFM1L	Thorlabs
11	Externally SM1-Threaded End Cap	1	SM1CP2	Thorlabs
12	Thorlabs mirror	2	BB1-E02	Thorlabs
13	30 mm Cage Right-Angle Kinematic Mirror Mount	2	KCB1	Thorlabs
14	XY Translating Lens Mount for Ø1″ Optics	1	CXY1	Thorlabs
15	SM1-Threaded Manual Beam Shutter, Ø7.2 mm Clear Aperture	1	SM1SH1	Thorlabs
16	Z-Axis Translation Mount, 30 mm Cage Compatible	1	SM1Z	Thorlabs
17	Aluminum Breadboard, 18″ × 18″ × 1/2″, 1/4″-20 Taps	1	MB2424	Thorlabs
18	Cage-Compatible, Cont. Variable, Refl. ND Filter Wheel, OD = 0-4.0, 8-32 Tap	1	NDM4	Thorlabs
19	FC/PC Adapter	1	SM1FC	Thorlabs
20	30 mm Cage Alignment Plate with Ø0.9 mm Hole	2	CPA1	Thorlabs
21	SM1-Threaded 30 mm Cage Plate	3	CP33	Thorlabs
22	Cage Assembly Rod, 1.5″ Long, Ø6 mm	2	ER1.5	Thorlabs
23	Cage Assembly Rod, 6″ Long, Ø6 mm	4	ER6	Thorlabs
24	Cage Assembly Rod, 12″ Long, Ø6 mm	2	ER12	Thorlabs
25	Ø1″ Pillar Post, 1/4″-20 Taps, L = 3″	1	RS3	Thorlabs
26	Adjustable-Height Platform for Ø1″ Posts, 1.75″ Adjustment Range	1	C1019	Thorlabs
27	Ø1/2″ Universal Post Holder, Spring-Loaded Locking Thumbscrew, L = 3″	5	UPH3	Thorlabs
28	Ø1/2″ Optical Post, SS, 8-32 Setscrew, 1/4″-20 Tap, L = 3″	5	TR3	Thorlabs

(*Continued*)

Table 1 Materials Needed to Build and Test the FLiP Set-Up (Basic Protocol 1), *continued*

#	Material[a]	# needed	Product number	Company
29	1/4″-20 Stainless Steel Cap Screw, 3/4″ Long, 25 Pack	1	SH25S075	Thorlabs
30	1/4″-20 Stainless Steel Setscrew, 3/4″ Long, 25 Pack	1	SS25S075	Thorlabs
31	SM1-Threaded 30 mm Cage Plate, 0.35″ Thick, 2 Retaining Rings, 8-32 Tap	2	CP02	Thorlabs
32	1″ Adjustable Lens Tube, External Threads, 0.5″ Long	1	SM1V05	Thorlabs
33	1″ Adjustable Lens Tube, External Threads, 1″ Long	2	SM1V10	Thorlabs
34	Tube Coupler, External Threads, 2″ Long	2	SM1T20	Thorlabs
35	Tube Coupler, External Threads, 1″ Long	1	SM1T10	Thorlabs
36	Tube Coupler, External Threads, 0.5″ Long	1	SM1T2	Thorlabs
37	SM1 Lens Tube, 1.00″	1	SM1L10	Thorlabs
38	Achromatic vis (A) coated lens, f = 30 mm	2	AC254-030-A-ML	Thorlabs
39	Ø1.25 mm Ferrule Adapter Plate with External SM1 Threads	1	SM1LCM	Thorlabs
40	Ceramic mating sleeve	1	ADAL1	Thorlabs
41	SM1 c-mount adapter	1	SM1A9	Thorlabs
42	Custom mount for laser base	1	-	Machine shop
43	Custom mount for laser front	1	-	Machine shop
44	Windows-based computer with at least two available PCI or PCIe slots (depending on choice of photon counting and detector controller board) + computer accessories	1	-	-
45	SMA cables, 24″	2	-	-
	Tools and accessories:			
46	Hex key set	1	CCHK	Thorlabs
47	Compact Power and Energy Meter Console, Digital 4″ LCD	1	PM100D	Thorlabs
48	Standard Photodiode Power Sensor, Si, 400-1100 nm, 50 mW	1	S120C	Thorlabs
49	Spanner Wrench for SM11-Threaded Retaining Rings	1	SPW602	Thorlabs
50	Blackout fabric	1	BK5	Thorlabs
51	Fine tape	1	-	-
	Optional:			
52	Oscilloscope	1	-	-
53	Trans-impedance amplifier	1	-	-
54	NI cards, e.g., PCI-6713 and PCI-6115, for pulse generation and recording of electrical signals using custom FLiP MATLAB software	1	PCI-6713, PCI-6115	NI

[a]Please note that similar components are available from other vendors and that products with similar functionality are also applicable to building this system.

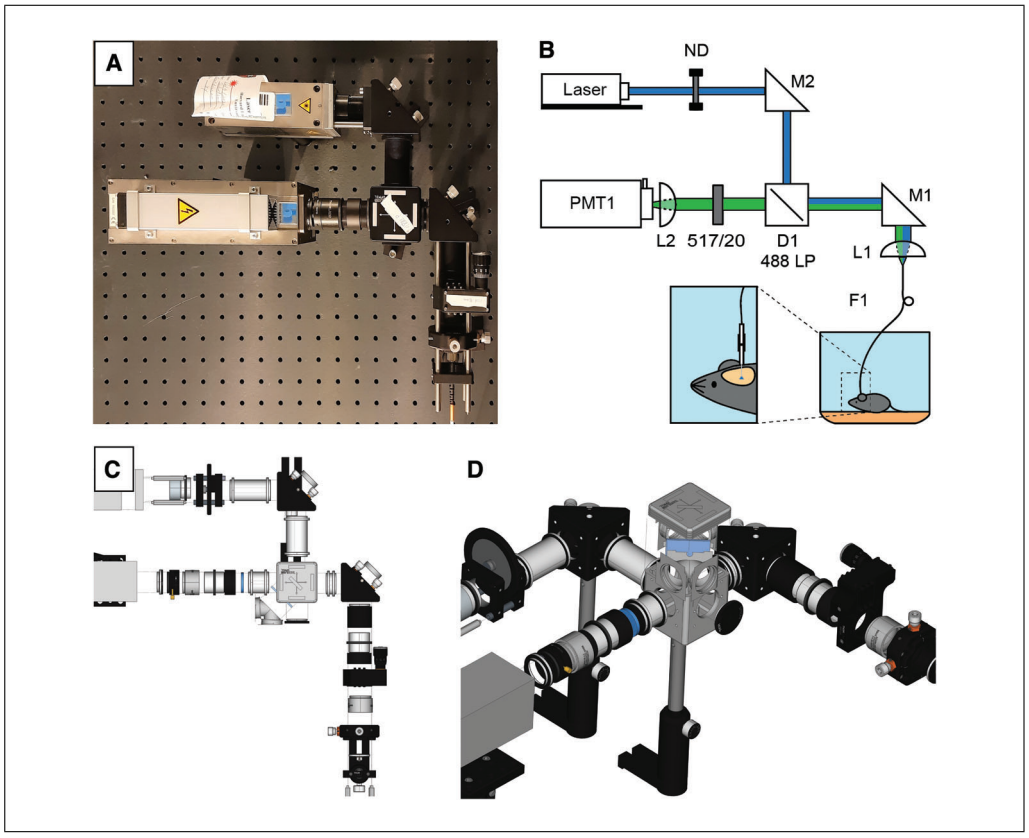

Figure 1 FLiP hardware overview. (**A**) Image of the FLiP system. This system lacks the rotatory ND filter, which is usually placed between the laser and M2. (**B**) Schematic of the FLiP system with the fiber optic attached to the mouse head. (**C**) 3D exploded model of the FLiP system, top view. (**D**) 3D exploded model of the FLiP system, side view. Figure 1B was modified from prior work (Lee et al., 2019).

9. Put broadband Thorlabs mirrors (12) into the right-angle kinematic mirror mounts (13) and put each mirror mount on a 0.5″ post (28) and post holder (27).
10. Screw a tube coupler (34, external threads, 2″ long) into open end of the mounted ND filter.
11. Designate one of the mirrors assembled in step 9 as M2. While supporting the M2 mirror, screw M2 post into the tube coupler; see Figures 1A and 1B. Make sure that M2 is directing light to the right. Secure M2 first using outer threaded rings by turning one toward the ND filter and one toward M2. Then, adjust height of the 0.5″ post of M2 and release support. Secure M2 post to the breadboard using a 1/4″-20 cap screw (29); see Figure 1B.
12. Take kinematic cube insert out of its base (10) and mount 488LP dichroic (8) into the insert. Make sure that reflective side of the dichroic (marked by Semrock with the name of the product) matches the reflection arrows as written on the top of the insert. Place insert back into the base.
13. Attach a 0.5″ post (28) and post holder (27) to the kinematic cube.
14. Screw a tube coupler (34, external threads, 2″ long) into open side of the M2 mirror and attach the kinematic cube to the other end in a similar fashion as discussed in step 11. Make sure that dichroic is oriented to direct the laser light to the left.
15. *IMPORTANT:* Before the next few steps, make sure that optics are well secured, both to each other (through external rings and tubes) and to the breadboard.

First alignment

16. To align the beam, secure two 12″-long (or 6″, depending on the choice of breadboard) 6-mm rods (24) to top two slots of the left opening of the kinematic cube. Slide an SM1-threaded 30-mm cage plate (31) on the rods and temporarily slide it close to kinematic cube.

17. Secure a second SM1-threaded 30-mm cage plate (31) to a 0.5″ post (28) and post holder (27). Slide this cage plate onto the two rods and move it close to kinematic cube. Secure post holder to the post to lock it in the proper post height. After securing the height, move cage plate with the post to ∼0.5″ away from the end of the long rods and secure it to breadboard with a 1/4″-20 screw (29). Secure other 30-mm cage plate at about one-fourth the distance between the kinematic cube and the cage plate with the post. Hang a cage alignment plate (20) on the rods against the 30-mm cage plates, with the target facing the laser side.

18. Turn laser on and change power to a level where the beam on the alignment plate can be clearly observed.

    Make sure to operate the laser safely in accordance with your institution's safety rules, including the use of laser safety goggles.

19. Check if laser beam hits the center on both alignment tools (in order to see the beam on the second alignment tool, temporarily take off the first). If the beam is not well centered on both alignment tools, change position and/or angle of the beam. Start with aligning beam on the *x*-axis: Take alignment tool closest to the kinematic cube off. Look on alignment tool farthest from the kinematic cube, and if the position of the beam is off center, correct it using M2. Then, place first alignment tool back in place and center beam on the first alignment tool using the fine adjustable screw. Repeat these steps until beam is in the center of both alignment tools. Next, align beam on the *y*-axis: Take out first alignment tool and adjust M2 to center beam on the second alignment tool.

    Observe that the mirror can be moved in three ways. The upper and lower adjuster knobs control the angle of the beam on the y-axis and x-axis, respectively. The fine screw in the bottom right corner, adjustable using a 5/64" hex, controls the position of the beam on the x-axis.

20. When the beam is centered, turn off laser, take cage plates off the 12″ rods, and take 12″ rods off the kinematic cube.

Assembly of the fiber launch

21. Designate remaining mirror assembled in step 9 as M1. Screw a tube coupler (36, external threads, 0.5″ long) into left side of the kinematic cube and attach M1 to other end in similar fashion as discussed in step 11. Make sure that M1 is directing laser light to the right.

22. To align the beam, first follow steps 16 to 19 using M1 instead of kinematic cube. Start with aligning beam on the *x*-axis: Look on alignment tool closest to M1, and if the position is off center, correct it using M2. Then, take this first alignment tool out and center beam on the second alignment tool using M1. Repeat these steps until beam is in the center of both alignment tools and then follow same steps to center on the *y*-axis.

    Both mirrors control the angle of the beam. However, the mirror closer to the source of the light (in our case, M2) has more impact on the position of the beam than the farthest mirror (M1).

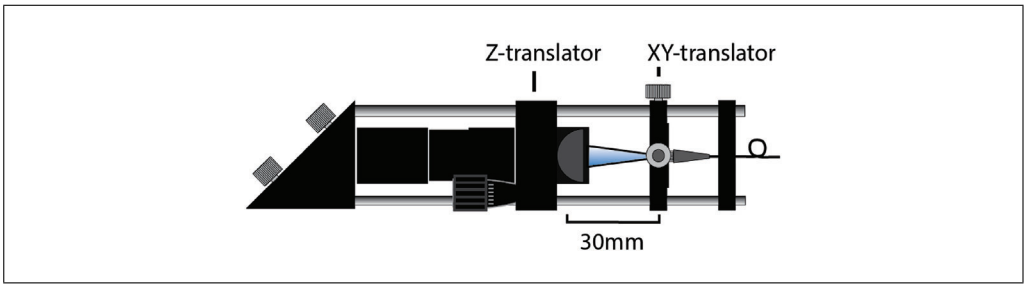

Figure 2 Detailed top view of the fiber launch referenced in steps 21 to 29 of Basic Protocol 1.

23. When the beam is centered, turn off laser, take cage plates off the 12″ rods, and take 12″ rods off M1.

24. Insert a 1″ adjustable lens tube (33, external threads, 1″ long) into an SM1 lens tube, 1.00″ (37), and screw it into open end of M1; see Figure 2.

25. Secure four 6″-long 6-mm rods (23) on open side of M1.

26. Attach a 30-mm-focal-length lens (38) to Z-translator (16) and put Z-translator on the rods in such a way that the curved side of the lens is facing toward the laser path. Make sure that lens is on the side of the Z-translator facing away from the laser, i.e., the part of the translator that moves; see Figure 2.

    You might need to take the lens out and reverse its orientation in the holder.

27. Screw and secure FC/PC adapter (19) into the XY-translator (14), check if XY-translator is centered, and place XY-translator onto the four rods at ∼30 mm from the lens, with the FC/PC slot facing away from the laser. Place an SM1 plate (21) onto a post (28) and place post into a post holder (27). Place SM1 plate (21) onto the end of the 6"-long rods, secure height, and screw it to breadboard to increase the stability of the set-up; see Figure 2.

28. Install computer (44), photon-counting board (5), and detector controller (4) in accordance with the instructions provided by the manufacturers. *Optional:* If using NI DAQ cards (54), install these as well.

Second alignment

29. Secure patch cord (6) into the FC/PC adapter and turn laser on in order to see if light is coming out of the patch cord. If light is coming out properly, turn laser off; otherwise, adjust XY-translator and Z-translator until light comes out of the fiber and then turn laser off.

    If the beam hits the center of the lens and is well collimated, then the light that exits the patch cord should be a filled circle. If you see a ring of light exiting the fiber, this indicates that the light is entering at an angle into the patch cord. Make sure not to stare directly into the fiber, but rather use a diffuse surface such as a non-reflective wall or a table.

30. To measure the light coming out of the patch cord, screw ferrule adapter (39) into an SM1-threaded 30-mm cage plate (21), screw SM1-threaded 30-mm cage plate onto the slim photodiode power sensor (48), and attach photodiode to the power meter (47). Connect patch cord to the optical power meter through the ferrule adapter. *Optional:* Connect power meter to a trans-impedance amplifier (53) and oscilloscope (52) to enhance the temporal resolution of power measurement in the next step.

31. Turn laser on. To put the patch cord entrance into the focus of the lens, change XY position (on the XY-translator) and Z position (by moving the XY-translator for course changes and Z-translator for finer changes) while simultaneously monitoring the optical power output of the patch cord on the power meter.

You may need to change the XY and Z components multiple times until the optimum spot is found. This step is important not only for the excitation path but also for the emission path.

32. When the patch cord is in the focus of the lens, secure all components. If through securing the components, the fiber moves slightly out of focus, correct for this by repeating step 32. If the entrance of the patch cord is in focus, turn off laser. *Optional:* Secure another patch cord (6) of similar length to set-up and tape it to the first patch cord using fine tape (51).

    During measurement, this patch cord can be attached to a dummy ferrule on the head of the mouse and secured with a piece of paper tape to ensure that the patch cord does not slip off while a mouse is performing behavior.

33. Cut out a piece of blackout fabric (50) and wrap it around fiber launch to make sure no light enters the set-up. Secure it with tape (51). *Optional:* Depending on the amount of ambient light during the recording of future experiments, put some blackout fabric around adjustable ND filter. However, make sure that filter will still be easily adjustable.

Assembly of the filter and detector

34. Place 517/20 filter (9) into the tube coupler (35, external threads, 1″ long) and secure filter using the filter-spanning wrench (49). Screw a tube coupler (35, external threads, 1″ long) into a 1″ adjustable lens tube (33, external threads, 1″ long) and attach it to right side of the kinematic cube. Attach an externally SM1-threaded end cap (11) on remaining opening of the kinematic cube.

35. Screw a 30-mm lens (38) onto tube and attach an SM1-threaded manual beam shutter (15). Attach SM1 c-mount adapter (41) to the SM1-threaded manual beam shutter.

36. Screw 1″ post (25, 3″ length) into the breadboard at the location where the PMT will be placed and place an adjustable-height platform (26) for Ø1″ posts on 1″ post but do not secure it yet.

37. Making sure to work in very-low-light conditions so that the hybrid PMT will not be damaged, take cap off the hybrid PMT (3) and, while supporting the PMT, screw SM1 c-mount adapter + SM1-threaded manual beam shutter + lens tightly on the PMT. Use one of the outer rings to tighten the construction and then, while continuing to support the PMT, raise adjustable-height platform for Ø1″ posts and secure it so that PMT base is supported. Check that SM1-threaded manual beam shutter is closed to protect the PMT before turning on the light.

38. Connect PMT to the detector controller board (4), as instructed by B&H.

Test the FLiP system using the B&H software

39. Connect laser reference and PMT to the time-correlated single-photon-counting (TCSPC) module as instructed by B&H.

    Please consider the length of the SMA cable (45) carrying the laser reference pulse, as described in more detail in step 45.

40. Install B&H software or use custom software to do the following:

    a. Perform continuous lifetime and photon count acquisition.
    b. Save lifetime histograms of individual acquisition time bins (e.g., 1 s).
    c. Export lifetime histograms for further analysis using a programming language.
    d. Display time-series data on photon counts and/or relative lifetime.

    See the B&H TCSPC manual for more information how to use the software.

41. Determine rate of photon counts needed for the application of interest.

    The photon-counting rate is the rate at which the FLiP system registers single photons detected by the PMT. The timing of these photons is recorded at high precision and eventually sent to the computer after acquisition. The minimal useful photon-counting rate depends on the temporal resolution of lifetime measurements needed to capture behavior-related changes at a certain signal-to-noise ratio, i.e., a certain number of photons needs to be measured to accurately estimate lifetime per time bin. To accurately estimate the sensor's lifetime, the required number of photons in a single time bin is usually between 5×10^4 and 5×10^5 photons, depending on the application. In addition, it is best to first determine the number of photons necessary to obtain a lifetime measurement with sufficient signal-to-noise and to then adjust to the illumination power to achieve that many photons in the behaviorally relevant time bin.

    Unfortunately, photon-counting rates cannot be increased indefinitely. At the extreme, at high light levels, the PMT will shut down or be damaged. However, this limit is typically not reached, as laser power should be kept considerably below these levels due to the maximum photon-counting rate of the TCSPC module, multi-photon excitation events, and photobleaching. Every TCSPC module has a maximum counting rate, which cannot be exceeded in order for the system to work properly. In addition, the goal in photon-counting lifetime measurements is to measure the time during which a single fluorophore is in the excited state before releasing a photon (Ebrecht, Don Paul, & Wouters, 2014). Therefore, the laser excitation power has to be kept low enough such that less than one photon is detected for each laser excitation pulse. Typically, the time measurement is made from the excitation pulse to the FIRST photon detected. For this reason, if more than one fluorophore is excited, the measured lifetime artificially drops. Finally, high laser power during measurements leads to photobleaching, and although lifetime imaging is relatively unaffected by photobleaching compared to intensity measurements, extreme levels of photon bleaching must be prevented in order to sustain high signal-to-noise levels. Practically, bleaching may occur at different rates for the sensor and for background sources of light (the tissue, optical fiber, and optical elements), each of which has its own fluorescence lifetime, and thus bleaching, may alter the measured lifetime.

    For example, we recorded FLIM-AKAR in freely moving animals using an SPC830 TCSPC counting board and used a rate of 700,000 to 800,000 photons per second, with 0.85-s time bins and a 0.15-s delay between each bin to allow for data transport by the TCSPC module. The laser power was set between 0.6 and 1 μW, measured at the tip of the patch cord, and we performed FLiP measurement for a maximum of 2 hr per day per mouse for 13 consecutive days, with minimal bleaching.

42. Measure power output of the patch cord using the power meter (47, 48) and set it at 0.1 μW.

    Make sure to remember where the boundary is where the rotational ND filter switches from the lowest ND mode to the highest ND mode in order to prevent overloading your PMT while adjusting the power in later steps.

43. Attach an optic fiber implant (7) to patch cord using a mating sleeve (40). Lower optic fiber implant into a fluorescent sample (e.g., 0.1 mM fluorescein solution) and cover fiber optic using blackout fabric (50) to protect the PMT against ambient light.

44. Start measuring photon counts while shutter remains closed. Then, slowly open shutter while monitoring the photon counts. Make sure that photon counts do not increase farther than the target to make sure not to damage the PMT. If photon counts increase further than the target, close shutter and decrease intensity of excitation light using the ND filter and repeat this step. If the photon counts are below the target, slowly increase excitation light intensity using the ND filter until the target is reached.

    Photon counts can be distorted by noise in the system.

45. Inspect lifetime histogram to see if the estimated fluorescence lifetime of the fluorescein standard is close to its published value. Minimize noise if necessary.

For FLiP, there are several factors that can contribute to the noise in the system. First, there is electrical noise, which can be minimized by reducing the amount of electrical equipment in the behavior room, by making a small faraday cage around sensitive equipment such as the PMT, and by ensuring that components are adequately grounded. Second, ambient light can enter the set-up and contribute to background noise. Shield the set-up with blackout materials or work in conditions with low ambient light to ensure low background optical noise. Test the light-proofing by passing a dim flashlight around the exterior of the light-proofing while monitoring PMT output (be careful not to illuminate the PMT directly!). Third, laser light hitting the entrance of the patch cord, the inner core of the patch cord, or the fiber optic implant and brain tissue produces autofluorescence, which will distort the sensor fluorescence lifetime measurements. In order to reduce the patch cord autofluorescence, use low-fluorescent patch cords, such as the one recommended here. Over time, a fiber might increase in autofluorescence. Repeatedly bleach the fiber using high-power laser light to mitigate this effect. In our set-up, we found that the junction between the optical set-up and the patch cord can be a significant source of autofluorescence. To separate this autofluorescence from the signal, we adjusted the length of the patch cord, which determines the delay from pulsed laser emission, fluorescence generation in the tissue, and fluorescence detection at the PMT (light travels at ∼1 ft/ns in vacuum and slows according to the index of refraction of the medium through which it propagates). At 50 MHz, we found a fiber of 3 m in length to be sufficient to separate the time between autofluorescence of the patch cord entrance from the sensor signal; however, our set-up has a different path length than the compact set-up shared in this protocol, so some optimization of patch cord length might be necessary. Similarly, the length of the SMA cable between the laser and the photon-counting board adds a delay and should be adjusted to ensure that the incoming photon count follows the laser reference pulse.

FLIM-AKAR VIRAL INJECTION AND FIBER IMPLANTATION FOR FLiP MEASUREMENT

BASIC PROTOCOL 2

This protocol will describe the viral injection of FLIM-AKAR (a PKA sensor) and fiber implantation in the nucleus accumbens core. As viral injection and fiber implantation have been described in detail previously and many labs performing in vivo research already use viral injection and fiber implantation in optogenetic and fiber photometry experimental pipelines, we will not cover this subject in depth, but rather focus on specific considerations related to FLIM-AKAR measurement and FLiP in general. For a more detailed view of viral injections and fiber implantation, please see prior work (Correia, Matias, & Mainen, 2017; Cui et al., 2014; see Current Protocols article; Jacob et al., 2018).

Additional Materials *(also see Table 2)*

Sterile water
Dental cement and/or glue

Stereotactic surgical stage (as standard in lab for fiber photometry or optogenetic surgeries or as directed by referenced protocols)
Sutures (optional)

Additional reagents and equipment for maxiprep and viral packaging; mouse housing, anesthesia, surgical preparation, and craniotomy; conventional viral injection and fiber implantation; and treatment of inflammation (if applicable)

NOTE: We describe general steps of the surgery. Specifics can be followed as described in the references mentioned in the introduction of this protocol. Any steps important for FLiP or injection of FLIM-AKAR will be described in detail.

NOTE: Part numbers referenced in this protocol can be found in Table 2.

Table 2 Materials Specifically Needed for PKA FLiP Measurement (Basic Protocol 2)

#	Material specifically needed for PKA FLiP measurement (in addition to those used for conventional viral injection and fiber implantation)	# needed	Product number	Company
1	Mouse with cre expressed in cells of interest (e.g., Drd1a-cre or Adora2a-cre) (Díaz-García et al., 2021).	1	-	e.g., MMRRC UC Davis
2	AAV-FLEX-FLIM-AKAR	1	60445	Addgene
3	AAV-FLEX-FLIM-AKART391A	1	60446	Addgene
4	Low autofluorescence optic implantable fiber	1	MFC_200/230-0.37_ 4.5 mm_MF1.25_FLT	Doric lenses
	Optional:			
5	Ø1.25 mm, 6.4 mm Long Ceramic Ferrules	1	CFLC126-10	Thorlabs
6	Metal head plate	1	90457A100	McMaster-Carr/ machine shop

1. Before starting surgery, perform maxiprep and send plasmid for packaging at a viral packaging facility.
2. After receiving the virus, dilute it using sterile water to achieve a titer of 2.15×10^{13} gc/ml and 7.67×10^{12} gc/ml for AAV-FLEX-FLIM-AKAR (2) and AAV-FLEX-FLIM-AKART391A (3), respectively. Aliquot and store at –80°C.
3. *Optional:* Make head-plate bars by cutting a 2 × 2–mm, 12″-long stainless steel plate (6) into 1″ plates.

   These head-plate bars can be glued onto the skull of a mouse and fit into a head restrainer for easy attachment of the patch cord to the fiber implant before behavioral experiments (see Basic Protocol 3).
4. Before starting surgery, put mouse (1) under anesthesia and place it on a stereotactic surgical stage.
5. Clear hair, cut skin, and expose skull.
6. Perform craniotomy with a drill.
7. Inject 300 nl AAV-FLEX-FLIM-AKAR or AAV-FLEX-FLIM-AKART391A aliquoted titer (see step 2) at 50 nl/min for measurement of PKA or for control experiments, respectively. For targeting the nucleus accumbens core, use the following coordinates: anteroposterior +1.2 mm, mediolateral ±1.3 mm relative to bregma, dorsoventral 4.1 mm below brain surface.

   See Commentary for more details.

   FLiP measurement requires a FRET pair (sensor) in which the fluorescence of the donor and acceptor minimally overlaps or, even better, where the acceptor fluorophore is dark, thus allowing emitted photons to come only from the FRET donor (i.e., in FLIM-FRET sensors). An example of this is the FLIM-AKAR sensor, which has been specifically designed with a dark acceptor fluorophore (Chen et al., 2014).

   We recommend lowering the injection needle to dorsoventral 4.2 mm below the brain surface and subsequently retracting the needle by 0.1 mm before injection to ease the injection of the virus in the underlying tissue.

8. After injection, place a low-autofluorescence optic implantable fiber (4) 0.2 mm above target site.

   We advise the use of low-autofluorescent optic fiber implants, such as the Doric Lenses implants suggested here. Autofluorescence of optic implants can be compared using photometry measurement of the patch cord with the optic fiber implant in a dark box or room.

9. *Optional:* If only one hemisphere is targeted, secure an additional dummy ferrule (5) using either dental cement or glue ∼5 mm from the active implant to increase stability during measurement.

   See also step 32 in Basic Protocol 1.

10. Secure fibers and head plate using dental cement and/or glue.

11. Close wound using dental cement or sutures.

12. Let mouse recover and wait ≥2 weeks for expression of viral construct (FLIM-AKAR) before measurement (see Basic Protocol 3). To prevent damage to the implants, make sure to place mouse in a cage where it cannot get stuck to metal bars. Inspect wound for any signs of inflammation or crusts indicating infection during the recovery period, which could weaken the adherence of glue and influence experimental results. When inflammation is detected, follow institutional regulations to properly treat the animal.

PERFORMING MEASUREMENTS USING FLiP

BASIC PROTOCOL 3

In this protocol, we will describe the steps necessary to perform FLiP measurements in vivo. As the protocol is focused on using FLiP to measure FRET-FLIM sensors generally and PKA specifically, we do not describe how to design or implement a behavioral task. Rather, we describe considerations for behavioral experiments, allowing the user to optimize their behavioral tasks for FLiP measurement. In addition, although we are describing FLiP usage in the context of a behavioral task, it is important to note that this set-up is versatile and can be used in combination with many other techniques, e.g., optogenetics, chemogenetics, in vivo pharmacological studies, and complex behavioral paradigms.

Some consideration is necessary for the design of a behavioral paradigm suitable for FLiP measurements. Due to relatively low temporal resolution, task behaviors should be modified in order to measure the critical components of behavior separately (see also Basic Protocol 1 for considerations on the temporal resolution of FLiP). In addition, other limitations with optical fiber–based behaviors, such as movement of the fiber during behavior or patch cord length, need to be considered. An example of a FLiP-compatible learning behavior in which behavioral components of cue, operant behavior, and reward are adequately separated is depicted in Figure 3.

Additional Materials *(also see Table 3)*

B&H software or custom FLiP software
Paper tape (optional)

CAUTION: Make sure that laser power is kept at a minimum in order to protect the PMT. Make sure to follow animal handling guidelines from your institution.

NOTE: Part numbers referenced in this protocol can be found in Table 3.

1. Open B&H software (see the B&H TCSPC handbook for details) or custom FLiP software (see GitHub: *https://github.com/bernardosabatinilab/fluorescence-lifetime-photometry*).

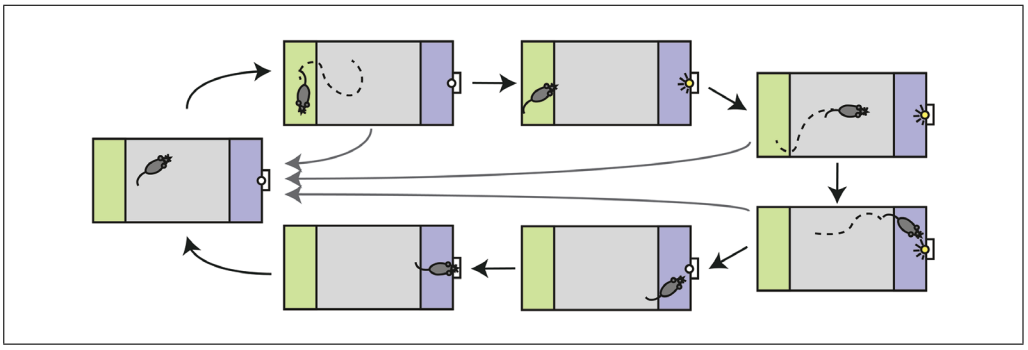

Figure 3 Temporally separated cue-directed operant conditioning task. In this behavior, freely moving mice can trigger a trial by walking into the trigger zone (depicted in green) and staying there for a period of 3 s. This will trigger the LED to turn on. Subsequently, the mouse will have 5 s to move into the receptacle zone (purple) and must stay there for a further 3 s in order to receive a food reward. If the mouse fails to reach the receptacle zone within 5 s or fails to stay in the receptacle zone for 3 s, the LED turns off, and the mouse will not receive a reward. Every trial is followed by an intertrial interval of 120 s, after which the next trial can be self-initiated. The figure was modified from prior work (Lee et al., 2020).

Table 3 Materials Necessary for Assessing Behavior Using FLiP (Basic Protocol 3)

#	Material	# needed	Product number	Company
1	Behavior box + equipment	1	-	-
2	Optional: Head restrainer	1	-	-
3	FLiP set-up	1	-	-
4	Ceramic mating sleeve	1	ADAL1	Thorlabs
5	Mouse injected with FLIM-AKAR	1	-	-
6	70% (v/v) ethanol wipes	1	-	-
7	Delicate task wipes	1	06-666A	Kimberly-Clark Professional

2. Attach a mating sleeve (4) to (each) patch cord.
3. Turn on laser from FLiP set-up from Basic Protocol 1 (3).
4. Restrain animal from Basic Protocol 2 (5), either by placing the mouse in a head restrainer (2) or by scruffing the mouse; see Figure 4.
5. Before connecting the fiber implant to the patch cord, clean top of the fiber implant using an ethanol wipe (6) and a delicate task wipe (7).
6. Connect patch cord(s) to the fiber implant (and dummy ferrule); see Figure 4B. *Optional:* If using two patch cords, tape mating sleeves together using paper tape for a lower risk of the patch cord falling off the implant during behavior.

   Disconnection of the patch cord not only disrupts the measurement but also risks damaging the hybrid PMT by allowing ambient light to be collected. Therefore, a lot of care must be taken in order to ensure that the patch cord does not fall off. Alternatively, observe the mouse while in behavior and uncoil the patch cord whenever necessary.
7. If not problematic for the behavioral experiment, place mouse in the behavioral box (1) so that the mouse has time to habituate before measurement.
8. While observing the photon counts in the B&H TCSPC software, slowly open PMT shutter to not overload the PMT and adjust ND filter in similar fashion as in step 44 of Basic Protocol 1.

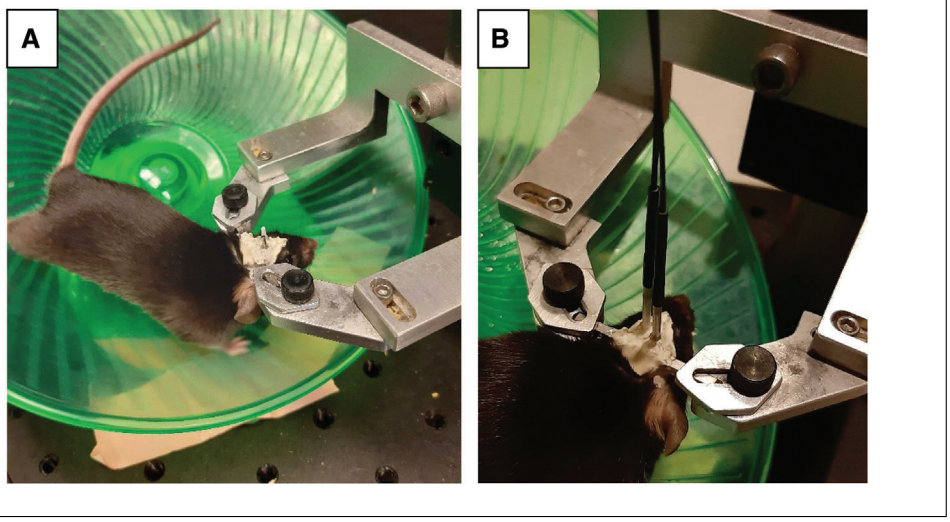

Figure 4 Head-fixed mouse. (**A**) The mouse is restrained by a head bar. (**B**) The patch cord is attached to the dummy and optical implant.

9. Start behavioral experiment and lifetime recording using the TCSPC software.

   See B&H TCSPC handbook for details.

10. Stop measurement when the behavioral experiment is finished.
11. Close shutter in front of the PMT.
12. Restrain mouse, as discussed in step 4 and detach patch cord from the mouse.

    In case of using paper tape, rip the paper close to the patch cord and peel the tape off. Be careful, as patch cords are sensitive.

13. Repeat steps 4 to 12 until all measurements have been completed.
14. Turn off laser and make sure that shutter in front of the PMT is closed.
15. Perform analysis using a custom script (also see Understanding Results).

COMMENTARY

Background Information

Over the past few decades, much progress has been made in understanding the mechanisms by which neuronal circuits control behavior. Observations of neural activity are generally achieved in behaving animals by electrical recordings with electrodes (Hong & Lieber, 2019) or monitoring Ca^{2+} entry into neurons with 2P microscopy (Díez-García, Akemann, & Knöpfel, 2007), endoscopic imaging (Ghosh et al., 2011), or fiber photometry (Cui et al., 2013). In addition, neural activity and signaling are manipulated with optogenetics (Boyden et al., 2005; Kim et al., 2017) and chemogenetics (Armbruster, Li, Pausch, Herlitze, & Roth, 2007; Roth, 2016). Less well understood and generally less accessible are the intracellular molecular mechanisms underlying changes in neuronal activity, cellular properties, and synaptic transmission, which occur during learning and behavioral adaptation. This is, in part, because of the difficulty of observing (and manipulating) biochemical changes in specific neurons in behaving animals. Although post hoc approaches have proven very helpful in understanding which genes, molecules, and signaling pathways were activated by a behavior, these analyses typically capture only slow and long-lasting molecular changes observed many minutes after the behavior of interest (Ramos et al., 2003).

Genetically encoded fluorescent sensors and reporters can be used to capture the transient and dynamic changes in the states of biochemical pathways during behavior. Such sensors include reporters for intracellular Ca^{2+} (Chen et al., 2013), which, although used as a surrogate for action potentials, is a second messenger; kinase activities or substrate

phosphorylation state (e.g., for CAMKII and PKA) (Chen et al., 2014; Erickson, Patel, Ferguson, Bossuyt, & Bers, 2011), or GTPases (e.g., Ras, Rac, Rho) (Bery et al., 2018; Boyden et al., 2005; Kim et al., 2017). Many of these reporters operate by exploiting FRET such that a biochemical cascade induces an intramolecular or intermolecular reorientation of two genetically encoded fluorophores, altering the fluorescence output of the acceptor and the acceptor fluorophore of a FRET pair.

2P FLIM is a powerful method to investigate biochemical changes in real time in individual neurons or even subcellular compartments. FLIM measures the fluorescence lifetime rate of fluorescence decay of the donor fluorophore of a FRET pair and thus directly accesses the molecular state of the FRET/FLIM sensor (Yasuda, 2018). For example, the FLIM-AKAR sensor is a sensor containing a FRET pair and a PKA phosphorylation substrate domain, which reports the net activity (balance between kinase and phosphatase) of a central kinase involved in plasticity, excitability, and gene expression. FLIM-AKAR contains a donor and dark-acceptor FRET pair, the components of which are brought in proximity due to phosphorylation by PKA, a process that is reversed by phosphatases. When donor and acceptor pairs are in proximity, FRET takes place, increasing the energy transfer between the donor and acceptor and thus reducing the fluorescence lifetime of the donor molecule (Chen et al., 2014). By collecting the fluorescence of the donor fluorophore and fitting a histogram of fluorescence lifetimes of many individual donor-fluorophore excitation events, FLIM measures the distribution between phosphorylated and unphosphorylated AKAR and, in principle, can estimate the absolute distribution of molecular states. In addition, 2P FLIM has a relatively fast temporal resolution ($\sim$1 s), has subcellular spatial resolution, and allows for easy manipulation of the sample within a microscope chamber. Recently, 2P lifetime imaging has been performed in vivo to measure molecular changes over time with single-neuron resolution (Díaz-García et al., 2017; Laviv et al., 2020; Ma et al., 2018). However, 2P FLIM also has disadvantages, such as the need to typically head-restrain an animal as well as the complexity and cost of the equipment. In order to perform bulk measurements of biochemical states in moving animals, we build on previous techniques to perform fluorescence lifetime measurements via fiber photometry (Cui et al., 2014) and have developed FLiP, a method that can measure molecular changes in vivo in real time using a single multimode fiber (Lee et al., 2019, 2020). In this article, we describe how to build a FLiP system (Basic Protocol 1), how to prepare mice for FLiP measurements (Basic Protocol 2), and how to perform the measurements in animals engaged in a behavioral task (Basic Protocol 3). As described in detail in the article, we have validated and used FLiP with the FLIM-AKAR sensor to measure PKA in vivo. However, many other FRET-FLIM sensors exist and are theoretically suitable for use with FLiP (Yasuda, 2018).

FLiP functions in a similar fashion as time-domain 2P FLIM, as it relies on single-photon excitation events to estimate the fluorescence lifetime of a sensor. A 473-nm laser emitting short light pulses (90 ps) at 50 MHz illuminates tissue in vivo through an optical fiber and is adjusted such that less than one emitted photon is detected by a PMT per laser pulse (in practice, we measure one photon per $\sim$100 laser pulses). Each photon hitting the photosensitive area of the PMT generates an electrical signal detected by the TCSPC module. The TCSPC board measures the delay between a reference signal generated by the laser when each light pulse is emitted and the single-photon detection by the PMT (Lee et al., 2019). The TCSPC module can record fluorescence lifetime at high speed, which is important, as the time delay between the excitation of the fluorophore and the emission of fluorescence is very short (usually on the scale of nanoseconds) and as many excitation events (about 50,000 to 500,000) are necessary to build a lifetime histogram allowing for accurate lifetime estimation; see Figure 5. The time needed to collect the number of individual excitation events necessary to accurately estimate lifetime generally determines the temporal resolution of the system.

FLiP offers several benefits compared to typical intensity-based ratiometric FRET measurements. A major confound of fiber photometry is the possibility of movement-generated changes in fluorescence, which are caused by fluctuations in intensity of fluorescence due to bending and jitter of the fiber in a freely behaving animal. As is true of all lifetime measurements, under FLiP, fluctuations in intensity are less of a concern, as the lifetime of the sensor is a single-molecule property and thus insensitive to the number of reporters excited or the efficiency with which their

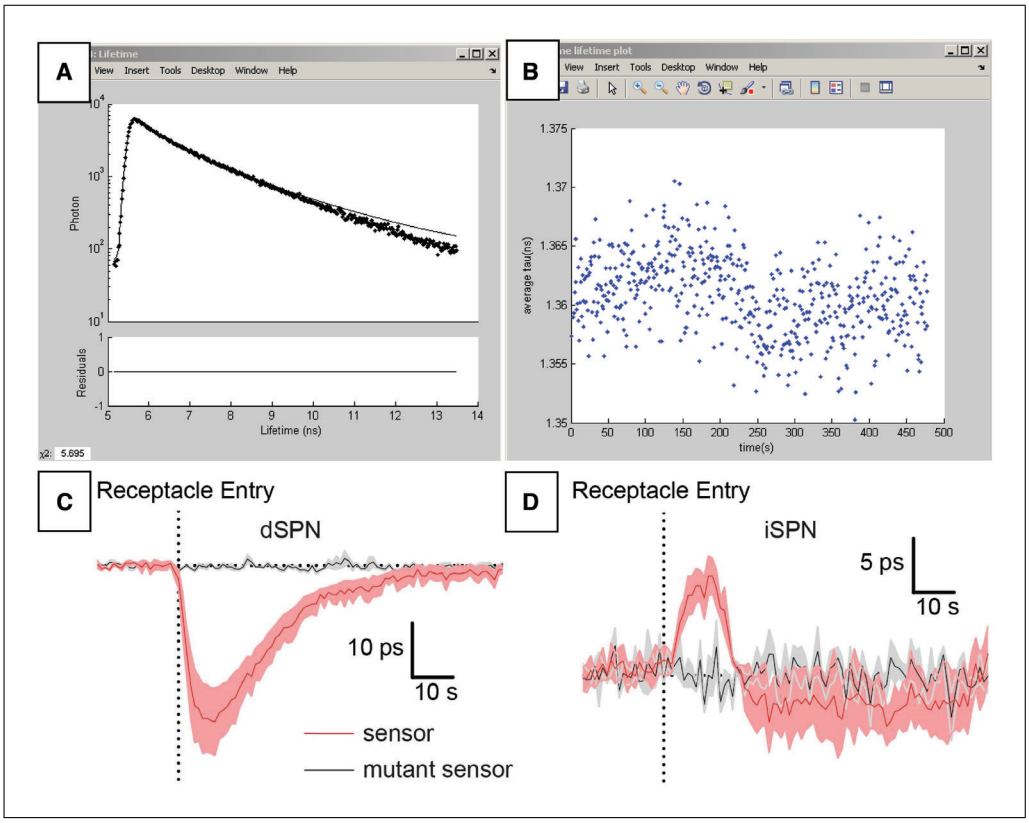

Figure 5 Examples of FLIM-AKAR traces measured using FLiP. (**A**) Fluorescence lifetime histogram with curve fit. (**B**) Lifetime can be recorded over time. (**C**) Food reward decreases the lifetime of FLIM-AKAR in D1R striatal projection neurons (dSPN) and does not change the lifetime of the mutant sensor (FLIM-AKART391A). (**D**) Food reward increases the lifetime of FLIM-AKAR in D2R striatal projection neurons (iSPN) and does not change the lifetime of the mutant sensor (FLIM-AKART391A). Figures 5C and 5D were reproduced from prior work (Lee et al., 2019).

fluorescence is detected. Of course, this only holds true as long as the sensor fluorescence is significantly greater than autofluorescence of the optical elements and unlabeled tissue. Additionally, FLiP uses very low imaging light (typically ~1 μW) and therefore causes significantly less photobleaching and phototoxicity. Furthermore, as FLiP relies on lifetime rather than intensity measurements, it is less sensitive to intensity change due to bleaching. Lastly, a FLIM sensor consisting of a donor fluorophore and a dark acceptor makes FLiP free of inherent challenges of a ratiometric FRET technique, which suffers from spectral overlap between the donor and acceptor fluorophore, differential photobleaching of the two fluorophores, and wavelength-dependent scattering, making accurate and stable measurement difficult. These benefits of FLiP allow for reliable measurement across many days.

Compared to 2P in vivo FLIM, FLiP has several advantages and disadvantages. FLiP is easy to implement and affordable, as the optics are not very different from those required in conventional fiber photometry and the electronic components are readily purchasable. FLiP also has significantly less photobleaching and phototoxicity compared to 2P in vivo FLIM. FLiP allows for a range of behavioral assays, as it can be easily used with both head-restrained and freely moving behaviors. Finally, FLiP can easily be used in combination with other in vivo strategies, such as optogenetics, fiber photometry, and freely moving behavioral assays (Lee et al., 2020). For example, to investigate the effect of the activity of genetically specified neuronal populations on intracellular signaling in another cell type in vivo, one can use a combination of FLiP and optogenetics. This can be done either using two separate fiber implants targeting separate regions or using a single fiber implant targeting the same region (which requires the simple addition of a dichroic mirror and a red-shifted laser to the current set-up) (Lee et al., 2020).

However, there are also some important limitations of FLiP. First, the temporal resolution (typically 100 ms per measurement) cannot be precisely controlled, as it is capped by

the maximum counting rate set by the TCSPC and the minimum number of single-photon measurements necessary to accurately estimate the reporter population lifetime. In addition, as opposed to 2P FLIM, in which autofluorescence can be negligible due to its ability to select the region of interest with a high level of sensor expression, the significant and variable autofluorescence in FLiP prevents measurements of the absolute fluorescence lifetime (Lee et al., 2019). However, FLiP does capture relative lifetime changes and thus relative biochemical changes, which is sufficient for most experimental purposes. Finally, FLiP is not an imaging approach and hence does not provide the spatial resolution of 2P FLIM; rather, it records the lifetime of many sensors across many neurons, as does fiber photometry.

Critical Parameters

There are several points in this set of protocols that require special attention and are key for a successful end result. In general, all optics and equipment should be handled carefully, as damage to any component in this system can disrupt successful measurements. More specifically, while building the FLiP system, pay special attention to aligning the beam correctly, as described in Basic Protocol 1. M1 not only is necessary for directing the light into the patch cord but also collects the emitted light. Therefore, if the beam is not well centered during the first alignment step after M2 is put in place, then M1 might have to compensate, causing the emission light to be off center and potentially miss the photocathode of the PMT. Additionally, make sure not to expose the hybrid PMT to ambient light, especially when it is turned on. High levels of light can seriously damage the PMT, and special care needs to be taken to protect it. While building, make sure to secure all components well, both to the breadboard and to each other, to ensure that the system remains stable long term. Always secure components before any alignment step, as the process can slightly change the angles and/or position of the optics. In addition, some optimization by the user might be required to ensure correct separation of autofluorescence and signal fluorescence, as described in the protocol, using modification of the length of the patch cord and laser pulse reference SMA cable. In addition, depending on the TCSPC module, signal-to-noise ratio, and temporal resolution desired for experiments, the user has to determine the photon count rate and temporal resolution appropriate for their application.

As with other techniques relying on stereotactic injection, a stable and reliable stereotactic surgical stage is necessary in order to target a particular anatomical site (Basic Protocol 2). Pay close attention to leveling the skull of the mouse and bregma approximation. Leveling tools are available for stereotactic surgeries, and we highly recommend investing in a system that supports these. For the expression of FLIM-AKAR, we have given recommendations of the viral titer, volume, and coordinates based on our own experiments. However, the viral titer and volume are suggestions and might need to be optimized for experiments targeting different regions and/or neuronal populations. We recommend performing test injections of different titers to find the optimal titer for each application. To prevent damaging the AAV-FLEX-FLIM-AKAR virus by repeated thawing and freezing, aliquot and store the virus at –80°C. Finally, to limit damaging brain tissue during fiber placement, slowly lower the optical fiber implant, as fast insertion increases tissue damage. The speed of implantation necessary to limit damage to the brain might vary per injection site. We typically lower the implant at ∼25 μm/s.

Successful use of FLiP (Basic Protocol 3) requires careful design of the experimental paradigm. Particularly important parameters are the predicted signal-to-noise ratio and the temporal resolution that will be achieved during measurement. The temporal resolution must be sufficient to capture the behavioral variables of interest during a task. If the signal-to-noise ratio is unknown or unpredictable, we recommend injecting a few animals to test the aforementioned variables before proceeding. During measurement, pay special attention to opening and closing the PMT shutter at appropriate times, as discussed in Basic Protocol 3. In addition, there might be slight variability between expression of FLIM-AKAR due to differences injection volume, targeting and variability across mice; therefore, the photon count might change mouse to mouse when measuring using a fixed laser intensity. For our applications, we increased the intensity of excitation light for each mouse until a specific number of photon counts per second was reached. As FLiP uses very-low-intensity light (∼1 μW), the variability in bleaching was minimal, and this practice ensured better signal-to-noise values for animals with relatively lower fluorescence intensity.

Troubleshooting

Please see Table 4 for potential problems and possible causes and solutions.

Understanding Results

Depending on the choice of software and type of measurement, there is limited opportunity to look at the lifetime change in real time. However, interpretation of the result is mainly done after analysis. For this, we recommend exporting the lifetime histogram bins (see Fig. 5) to MATLAB or Python and creating a custom script for analysis. An example of a custom script analyzing lifetime can be found on GitHub (*https://github.com/bernardosabatinilab/fluorescence-lifetime-photometry*). As mentioned above, FLiP does not support absolute lifetime measurements and can only capture relative lifetime change. The average lifetime of each acquisition time bin can be calculated using the formula displayed below, as discussed previously (Lee et al., 2009):

$$\tau_m| = < t > -t_0 = \frac{\int dt \cdot tF\,(t)}{dt.F\,(t)} - t_0$$

F(t) is the photon count of a fluorescence lifetime at time bin t, and t_0 is the offset of the lifetime histogram, which can be estimated from a double exponential fit to the lifetime histogram at the beginning of the analysis (Lee et al., 2019). After calculating the average lifetime of each acquisition time bin, subtract the average lifetime value of the baseline time period (reference period) to acquire the relative change in lifetime and align the average lifetime trace to the behavioral, pharmacological, or optogenetic event(s). Examples of lifetime traces during measurement of FLIM-AKAR fluorescence lifetime can be seen in Figure 5B. FLIM-AKAR relative lifetime data aligned to a mouse receiving a food reward for D1R and D2R striatal projection neurons can be found in Figures 5C and 5D, respectively.

The interpretation of lifetime change depends on the sensor. As mentioned in the Background Information section, the fluorescence lifetime of a FLIM sensor depends on the proximity of the donor fluorophore to the acceptor fluorophore domain. The FLIM-AKAR sensor contains a PKA substrate, which upon phosphorylation induces conformational changes leading to a reduced distance between the donor and acceptor. This proximity increases FRET efficiency, which lowers the fluorescence lifetime of the donor fluorophore (Chen et al., 2014). In addition, phosphatases can dephosphorylate FLIM-AKAR, which increases the average lifetime. Thus, changes in lifetime reflect the balance between PKA and phosphatase activity.

In order to be confident that the measurement is reflecting true biological change of the intended target, we recommend using the following controls:

One of the more straightforward ways to check if the sensor and FLiP are working is the use of systemic antagonists and/or agonists. Of importance here is that the drugs should specifically target the biological pathway of interest and that they can reach the target brain area upon systemic administration (note that some drugs often used in slice experiments do not effectively reach the brain upon systemic administration). In addition, as drugs often give a supra-physiological response, antagonists and agonists can be used to estimate the dynamic range of a sensor in vivo.

In order to control for cell viability, investigate cell death after an in vivo experiment. Cell death can be determined by investigating the morphology of transfected cells on histological slides of the fixed brain slices using epifluorescent microscopy. Consider lowering the titer if significant cell death is found.

In order to control for the specificity of expression, for example when trying to only transfect a particular cell population using the cre-lox system, immunohistochemistry of specific cellular markers prevalent in the cell population of interest may be performed. Comparison of the sensor fluorescence of the sample and the immunohistochemistry will allow investigation of the specificity of expression as well as quantify the fraction of the population expressing the sensor.

When using FLiP with a newly developed FRET-FLIM sensor, it is important to establish that the modulation of the sensor fluorescence reflects a specific biological change. Even though using systemic drugs is one way of answering this question, systemic drugs are often not specific enough to exclude other pathways or conditions. Therefore, one can exploit two strategies to gain confidence in the specificity of the sensor in vivo. First, use a genetically targeted inhibitor of the biological pathway of interest in order to establish the specificity of the sensor. In order perform this control, first inject a sensor virus and wait until the sensor expression is strong (determined in previous experiments). Then, inject a virus containing a construct for a cell type–specific and pathway-specific genetically targeted inhibitor and implant a fiber above the

Table 4 Troubleshooting Guide for PKA Activity Measurement Using FLiP

Problem	Possible cause	Solution
Mouse dies during or after surgery	Too much isoflurane during surgery	Lower isoflurane during surgery to make the mouse breathe at ∼1 Hz
	Improper analgesic administration	When using injectable analgesics, make sure that the proper method of administration is used. For analgesics in food, make sure that the mouse eats the food before and after surgery.
	Fiber implant damaged a critical structure (e.g., a blood vessel)	Investigate the brain for any irregularities. If damage is detected, consider injection and/or fiber implantation at an angle.
No/very low photon counts detected during fluorescein standard measurement	Hardware dysfunction	Closely examine the instructions and TCSPC handbook. Contact B&H if the problem cannot be identified.
	Damaged patch cord	Check the integrity of the patch cord by checking its transmission rate using the power meter. Replace the patch cord if damage is confirmed.
	Improper connection between the patch cord and implant	Make sure to properly connect the patch cord and implant by slightly turning the patch cord while gently attaching it to the ferrule implant on the mouse head. Make sure that there is enough room on the implanted ferrule to allow for patch cord/sleeve attachment.
Distorted lifetime histogram	Overlap between the autofluorescence arising from the entrance of the patch cord and the signal of the FLIM-AKAR sensor	Separate the autofluorescence and signal from the FLIM-AKAR sensor by changing the length of the patch cord
High PMT dark count (with closed PMT shutter)	Electrical noise induced by the environment triggers the PMT	Cover the PMT fully using a non-conductive material, followed by grounded aluminum foil. Make sure that the aluminum foil does not touch the PMT directly. Ground the aluminum foil to a grounding source.
		High temperatures can increase the dark count of a PMT. Make sure that the PMT operates under room-temperature conditions using a cooling mechanism.
High background photon count (with open PMT shutter)	Autofluorescence of the patch cord	Bleach the patch cord and fiber implant using a high-power blue (∼473 nm) laser before use.
	Ambient light enters the system and triggers the PMT	Check if all aspects of the set-up are well covered using blackout fabric
		Work in low-light conditions
Low photon counts during measurement	Repeated freezing and thawing resulting in degradation of virus	Make aliquots of the virus and check the stability of the –80°C storage facility
	Low viral titer	Test multiple titers and perform histological analysis to establish the appropriate titer for the application
	Incorrect virus injection and fiber placement	After completing in vivo experiments, perform histological analysis of the brain tissue to estimate the error in virus injection and fiber placement. Update the coordinates accordingly.

target site. Subsequently, measure the effect of pharmacological agonists/antagonists in a sequential manner (Lee et al., 2019). If the effect of the pharmacological drug diminishes as the expression level of the inhibitor virus increases, then this is a good indication that the sensor is specific to the change in the target biological pathway. Second, in order to control for optical artifacts and off-target effects on the sensor, use a mutant sensor in which the consensus active site specific to the biological mechanism of interest (e.g., the PKA substrate domain of FLIM-AKAR) is mutated. Inject the virus containing the construct of this genetically targeted mutant sensor instead of the functional sensor and perform FLiP to observe, using pharmacological or biological experiments, if the signal previously observed is preserved. If not, then this is a good indication that the FLiP system is working and that the sensor is specific.

Time Considerations

Basic Protocol 1: 1 week.

Basic Protocol 2: 1.5 to 3 hr

Basic Protocol 3: 20 min to 2 hr, depending on the specific behavioral task.

Acknowledgments

This work was supported by the NIH (B.L.S., R37NS046579), Howard Hughes Medical Institute (B.L.S.), Sackler Scholar Program in Psychology (S.J.L.), Schuurman Schimmel van Outeren Stichting (B.L.), Hendrik Muller Fonds (B.L.), and Boehringer Ingelheim Foundation (B.L).

Author Contributions

Bart Lodder: Writing-original draft. **Suk Joon Lee**: Writing-original draft. **Bernardo Sabatini**: Writing-original draft.

Conflict of Interest

The authors declare no conflict of interest.

Data Availability Statement

Data available on request from the authors.

Literature Cited

Armbruster, B. N., Li, X., Pausch, M. H., Herlitze, S., & Roth, B. L. (2007). Evolving the lock to fit the key to create a family of G protein-coupled receptors potently activated by an inert ligand. *Proceedings of the National Academy of Sciences of the United States of America*, *104*(12), 5163–5168. doi: 10.1073/pnas.0700293104.

Barretto, R. P. J., Messerschmidt, B., & Schnitzer, M. J. (2009). *In vivo* fluorescence imaging with high-resolution microlenses. *Nature Methods*, *6*(7), 511–512. doi: 10.1038/nmeth.1339.

Bery, N., Cruz-Migoni, A., Bataille, C. J., Quevedo, C. E., Tulmin, H., Miller, A., … Rabbitts, T. H. (2018). BRET-based RAS biosensors that show a novel small molecule is an inhibitor of RAS-effector protein-protein interactions. *eLife*, *7*, e37122, doi: 10.7554/elife.37122.

Boyden, E. S., Zhang, F., Bamberg, E., Nagel, G., & Deisseroth, K. (2005). Millisecond-timescale, genetically targeted optical control of neural activity. *Nature Neuroscience*, *8*(9), 1263–1268. doi: 10.1038/nn1525.

Chen, T. W., Wardill, T. J., Sun, Y., Pulver, S. R., Renninger, S. L., Baohan, A., … Kim, D. S. (2013). Ultrasensitive fluorescent proteins for imaging neuronal activity. *Nature*, *499*(7458), 295–300. doi: 10.1038/nature12354.

Chen, Y., Saulnier, J. L., Yellen, G., & Sabatini, B. L. (2014). A PKA activity sensor for quantitative analysis of endogenous GPCR signaling via 2-photon FRET-FLIM imaging. *Frontiers in Pharmacology*, *5*, 56. doi: 10.3389/fphar.2014.00056.

Correia, P., Matias, S., & Mainen, Z. (2017). Stereotaxic adeno-associated virus injection and cannula implantation in the dorsal raphe nucleus of mice. *Bio-protocol*, *7*(18), e2549. doi: 10.21769/bioprotoc.2549.

Cui, G., Jun, S. B., Jin, X., Luo, G., Pham, M. D., Lovinger, D. M., … Costa, R. M. (2014). Deep brain optical measurements of cell type-specific neural activity in behaving mice. *Nature Protocols*, *9*(6), 1213–1228. doi: 10.1038/nprot.2014.080.

Cui, G., Jun, S. B., Jin, X., Pham, M. D., Vogel, S. S., Lovinger, D. M., & Costa, R. M. (2013). Concurrent activation of striatal direct and indirect pathways during action initiation. *Nature*, *494*(7436), 238–242. doi: 10.1038/nature11846.

Díaz-García, C. M., Meyer, D. J., Nathwani, N., Rahman, M., Martínez-François, J. R., & Yellen, G. (2021). The distinct roles of calcium in rapid control of neuronal glycolysis and the tricarboxylic acid cycle. *eLife*, *10*, 1–30. doi: 10.7554/eLife.64821.

Díaz-García, C. M., Mongeon, R., Lahmann, C., Koveal, D., Zucker, H., & Yellen, G. (2017). Neuronal stimulation triggers neuronal glycolysis and not lactate uptake. *Cell Metabolism*, *26*(2), 361–374.e4. doi: 10.1016/j.cmet.2017.06.021.

Díez-García, J., Akemann, W., & Knöpfel, T. (2007). *In vivo* calcium imaging from genetically specified target cells in mouse cerebellum. *NeuroImage*, *34*(3), 859–869. doi: 10.1016/j.neuroimage.2006.10.021.

Ebrecht, R., Don Paul, C., & Wouters, F. S. (2014). Fluorescence lifetime imaging microscopy in the medical sciences. *Protoplasma*, *251*(2), 293–305. doi: 10.1007/s00709-013-0598-4.

Erickson, J. R., Patel, R., Ferguson, A., Bossuyt, J., & Bers, D. M. (2011). Fluorescence resonance energy transfer-based sensor camui provides new insight into mechanisms of calcium/calmodulin-dependent protein kinase II

activation in intact cardiomyocytes. *Circulation Research*, *109*(7), 729–738. doi: 10.1161/CIRCRESAHA.111.247148.

Ghosh, K. K., Burns, L. D., Cocker, E. D., Nimmerjahn, A., Ziv, Y., Gamal, A. El, & Schnitzer, M. J. (2011). Miniaturized integration of a fluorescence microscope. *Nature Methods*, *8*(10), 871–878. doi: 10.1038/nmeth.1694.

Goto, A., Nakahara, I., Yamaguchi, T., Kamioka, Y., Sumiyama, K., Matsuda, M., … Funabiki, K. (2015). Circuit-dependent striatal PKA and ERK signaling underlies rapid behavioral shift in mating reaction of male mice. *Proceedings of the National Academy of Sciences of the United States of America*, *112*(21), 6718–6723. doi: 10.1073/pnas.1507121112.

Hong, G., & Lieber, C. M. (2019). Novel electrode technologies for neural recordings. *Nature Reviews Neuroscience*, *20*(6), 330–345. doi: 10.1038/s41583-019-0140-6.

Iino, Y., Sawada, T., Yamaguchi, K., Tajiri, M., Ishii, S., Kasai, H., & Yagishita, S. (2020). Dopamine D2 receptors in discrimination learning and spine enlargement. *Nature*, *579*(7800), 555–560. doi: 10.1038/s41586-020-2115-1.

Jacob, A. D., Ramsaran, A. I., Mocle, A. J., Tran, L. M., Yan, C., Frankland, P. W., & Josselyn, S. A. (2018). A compact head-mounted endoscope for *in vivo* calcium imaging in freely behaving mice. *Current Protocols in Neuroscience*, *84*(1), e51. doi: 10.1002/CPNS.51.

Kebabian, J. W., Petzold, G. L., & Greengard, P. (1972). Dopamine-sensitive adenylate cyclase in caudate nucleus of rat brain, and its similarity to the "dopamine receptor". *Proceedings of the National Academy of Sciences of the United States of America*, *69*(8), 2145–2149. doi: 10.1073/pnas.69.8.2145.

Kim, C. K., Adhikari, A., & Deisseroth, K. (2017). Integration of optogenetics with complementary methodologies in systems neuroscience. *Nature Reviews Neuroscience*, *18*(4), 222–235. doi: 10.1038/nrn.2017.15.

Lau, G. C., Saha, S., Faris, R., & Russek, S. J. (2004). Up-regulation of NMDAR1 subunit gene expression in cortical neurons via a PKA-dependent pathway. *Journal of Neurochemistry*, *88*(3), 564–575. doi: 10.1046/j.1471-4159.2003.02156.

Laviv, T., Scholl, B., Parra-Bueno, P., Foote, B., Zhang, C., Yan, L., … Yasuda, R. (2020). *In vivo* imaging of the coupling between neuronal and CREB activity in the mouse brain. *Neuron*, *105*(5), 799–812.e5. doi: 10.1016/j.neuron.2019.11.028.

Lee, H. K., Takamiya, K., Han, J. S., Man, H., Kim, C. H., Rumbaugh, G., … Huganir, R. L. (2003). Phosphorylation of the AMPA receptor GluR1 subunit is required for synaptic plasticity and retention of spatial memory. *Cell*, *112*(5), 631–643. doi: 10.1016/S0092-8674(03)00122-3.

Lee, S. J., Chen, Y., Lodder, B., & Sabatini, B. L. (2019). Monitoring behaviorally induced biochemical changes using fluorescence lifetime photometry. *Frontiers in Neuroscience*, *13*, 766. doi: 10.3389/fnins.2019.00766.

Lee, S. J., Lodder, B., Chen, Y., Patriarchi, T., Tian, L., & Sabatini, B. L. (2020). Cell-type-specific asynchronous modulation of PKA by dopamine in learning. *Nature*, *590*(7846), 451–456. doi: 10.1038/s41586-020-03050-5.

Lee, S. J. R., Escobedo-Lozoya, Y., Szatmari, E. M., & Yasuda, R. (2009). Activation of CaMKII in single dendritic spines during long-term potentiation. *Nature*, *458*(7236), 299–304. doi: 10.1038/nature07842.

Linden, D. J., & Ahn, S. (1999). Activation of presynaptic cAMP-dependent protein kinase is required for induction of cerebellar long-term potentiation. *Journal of Neuroscience*, *19*(23), 10221–10227. doi: 10.1523/jneurosci.19-23-10221.1999.

Ma, L., Jongbloets, B. C., Xiong, W. H., Melander, J. B., Qin, M., Lameyer, T. J., … Zhong, H. (2018). A highly sensitive a-kinase activity reporter for imaging neuromodulatory events in awake mice. *Neuron*, *99*(4), 665–679.e5. doi: 10.1016/j.neuron.2018.07.020.

Nagai, T., Yoshimoto, J., Kannon, T., Kuroda, K., & Kaibuchi, K. (2016). Phosphorylation signals in striatal medium spiny neurons. *Trends in Pharmacological Sciences*, *37*(10), 858–871). doi: 10.1016/j.tips.2016.07.003.

Nayak, A., Zastrow, D. J., Lickteig, R., Zahniser, N. R., & Browning, M. D. (1998). Maintenance of late-phase LTP is accompanied by PKA-dependent increase in AMPA receptors synthesis. *Nature*, *394*(6694), 680–683. doi: 10.1038/29305.

Ramos, B. P., Birnbaum, S. G., Lindenmayer, I., Newton, S. S., Duman, R. S., & Arnsten, A. F. T. (2003). Dysregulation of protein kinase A signaling in the aged prefrontal cortex: New strategy for treating age-related cognitive decline. *Neuron*, *40*(4), 835–845. doi: 10.1016/S0896-6273(03)00694-9.

Roth, B. L. (2016). DREADDs for neuroscientists. *Neuron*, *89*(4), 683–694. doi: 10.1016/j.neuron.2016.01.040.

Skeberdis, V. A., Chevaleyre, V., Lau, C. G., Goldberg, J. H., Pettit, D. L., Suadicani, S. O., … Zukin, R. S. (2006). Protein kinase A regulates calcium permeability of NMDA receptors. *Nature Neuroscience*, *9*(4), 501–510. doi: 10.1038/nn1664.

Tang, S., & Yasuda, R. (2017). Imaging ERK and PKA activation in single dendritic spines during structural plasticity. *Neuron*, *93*(6), 1315–1324.e3. doi: 10.1016/j.neuron.2017.02.032.

Yagishita, S., Hayashi-Takagi, A., Ellis-Davies, G. C. R., Urakubo, H., Ishii, S., & Kasai, H. (2014). A critical time window for dopamine actions on the structural plasticity of dendritic spines. *Science*, *345*(6204), 1616–1620. doi: 10.1126/science.1255514.

Yasuda, R. (2018). Principle and application of fluorescence lifetime imaging for neuroscience: Monitoring biochemical signaling in single synapses using fluorescence lifetime imaging. In R. R. Alfano & L. Shi (Eds.), *Neurophotonics and Biomedical Spectroscopy* (pp. 53–64). Elsevier. doi: 10.1016/B978-0-323-48067-3.00003-2.

Zhang, X., Nagai, T., Ahammad, R. U., Kuroda, K., Nakamuta, S., Nakano, T., … Kaibuchi, K. (2019). Balance between dopamine and adenosine signals regulates the PKA/Rap1 pathway in striatal medium spiny neurons. *Neurochemistry International*, *122*, 8–18. doi: 10.1016/j.neuint.2018.10.008.